International Journal of Drug Design and Discovery

***Volume* 5 ● *Issue* 1 ● *January – March* 2014. 1276-1284**

Pharmacophore Modeling and Virtual Screening Studies on Colony Stimulating Factor 1 Receptor (CSF1R) Inhibitors

Pavan Kumar Machiraju[1,2]*, Jagarlapudi A.R.P. Sarma[1], K.R.S. Sambasiva Rao[2] and Rambabu gundla[1]

[1]*GVK Bio sciences Pvt. Ltd., Plot No. 79, IDA, Mallapur, Hyderabad-500076.*

[2]*Department of Biotechnology, Acharya Nagarjuna University, Nagarjuna Nagar, Guntur, AP, India.*

ABSTRACT: CSF-1R is a member of the class III receptor tyrosine kinases, along with c-Kit, Flt3, and PDGFR α and β. Colony stimulatory factor 1 (CSF-1), also known as macrophage/monocyte colony stimulatory factor (M-CSF), binds to CSF-1R, resulting in dimerization, autophosphorylation, and activation of signal transduction. To identify potent inhibitors against CSF-1R we deployed rational approaches of drug discovery. In current study, pharmacophore models were generated using a set of 118 structurally diverse compounds out of which 19 were chosen as training set and 99 as test set with an inhibitory activity ranging from 0.4 to 2100 ηM . The model was further validated using a test set of 99 compounds and got a correlation of 0.75. Virtual screening was performed using validated pharmacophore query against inhouse database of 20,000 compounds. Docking analysis was performed for a set of virtual hits with high predictive activity and structural diversity using Glide. Docking was performed in order to study the binding orientation and determine productive interactions within the active site. 12 hits were selected for pharmacological screening.

KEYWORDS: CSF-1R, Discovery Studio 3.0, 3D QSAR, Hypo 1, BAS12532928.

Introduction

CSF-1R, member of the class III receptor tyrosine kinases, along with c-Kit, Flt3 and PDGFR alpha and beta. Colony stimulatory factor 1 (CSF-1), also known as macrophage/monocyte colony stimulatory factor (M-CSF), binds to CSF-1R[1]. CSF1 and CSF-1R regulates cell survival, proliferation, differentiation and mononuclear phagocyte lineage[2-5]. CSF-1 binds to the extracelluar domain of induces dimerization and trans-autophosphorylation of the intracellular CSF-1R kinase domain[6]. Macrophages play an important role in several diseases, including cancer and inflammation, increased levels of macrophages best correlate with severity of the disease. Expression of CSF-1R in breast cancer has been linked to poor survivability and increased tumor size, where presumably the receptor is involved in local invasion and metastasis[7]. High levels of CSF-1 and CSF-1R have been identified in several tumor types, like endometrial, ovarian and breast cancers, and have also been related to invasion and metastasis. Inhibitions of CSF-1R activity have multiple effects on the tumor through reduction in the levels of tumor-associated macrophages[8].

* *For correspondence:* Pavan Kumar Machiraju
Email: pavan.machiraju@gvkbio.com

In this current study, we have generated pharmacophore model using known CSF1R inhibitors (training set) to identify a hypothetical model that contains crucial chemical features which are responsible for its biological activity. The generated pharmacophore model was validated using 99 CSF1R inhibitors (test set). Virtual screening was performed against inhose database of 20,000 compounds using the validated pharmacophore model. Top hits were selected from the screening based on its estimated activities/fit values. This hits were subjected for docking against CSF1R. Top hits were selected based on its pharmacophore fit values, docking analysis, hydrogen bond interactions for screening against CSF1R.

Materials and Methods

Selection of Molecules

A pharmacophore model contains collection of 3D spatial arrangement of features necessary for the biological activity. For the pharmacophore modeling studies, a set of 118 CSF1R inhibitors having IC_{50} spanning over 4 orders of magnitude (0.4 to 2100 ηM) was selected from the literature[7-10]. The training set is selected in such a way that considering both structural diversity and activity range. The most active, moderately active and inactive compounds were included in order to obtain a good

pharmacophore model (**Scheme-1**). The set 19 compounds was selected as a training set for model generation. To validate our pharmacophore, the remaining 99 compounds were used as the test set.

Scheme 1 Chemical structures 19 training set molecules applied to HypoGen for pharmacophore generation.

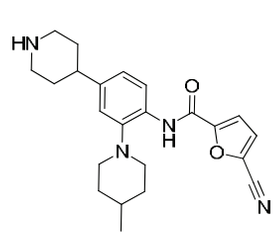

Moecule-1
IC_{50} = 0.3 nM

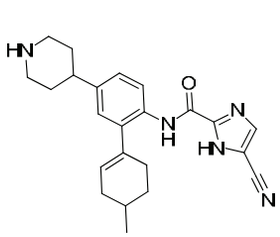

Moecule-2
IC_{50} = 0.4 nM

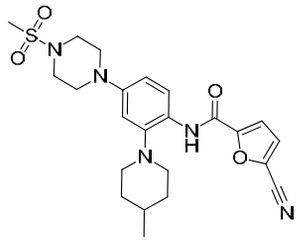

Moecule-3
IC_{50} = 0.9 nM

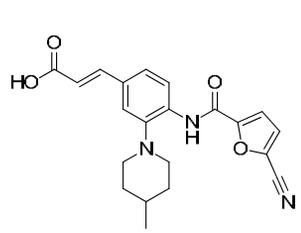

Moecule-4
IC_{50} = 2 nM

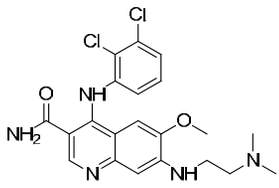

Moecule-5
IC_{50} = 3 nM

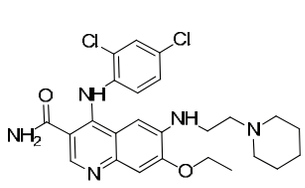

Moecule-6
IC_{50} = 6 nM

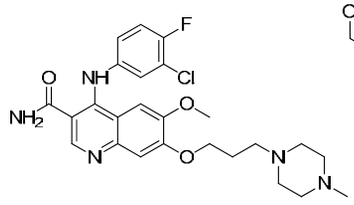

Moecule-7
IC_{50} = 7 nM

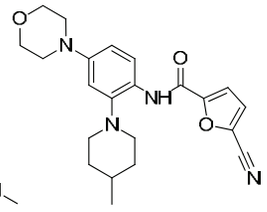

Moecule-8
IC_{50} = 11 nM

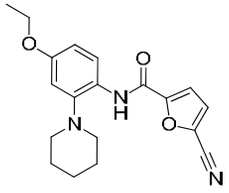

Moecule-9
IC_{50} = 21 nM

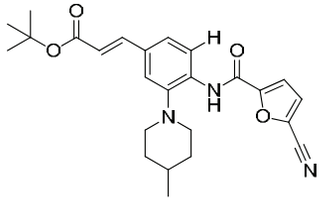

Moecule-10
IC_{50} = 38 nM

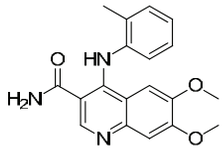

Moecule-11
IC_{50} = 52 nM

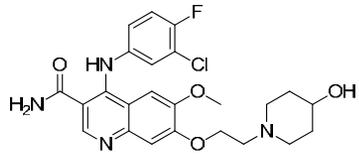

Moecule-12
IC_{50} = 80 nM

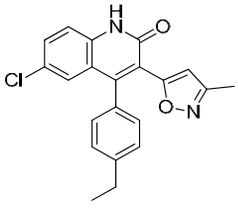

Moecule-13
IC_{50} = 90 nM

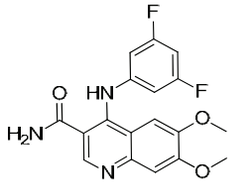

Moecule-14
IC_{50} = 100 nM

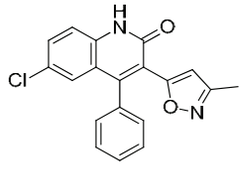

Moecule-15
IC_{50} = 140 nM

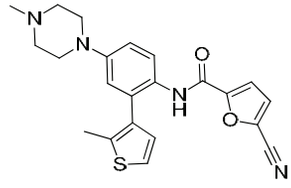

Moecule-16
IC_{50} = 470 nM

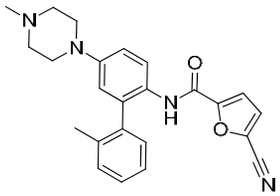

Moecule-17
IC_{50} = 630 nM

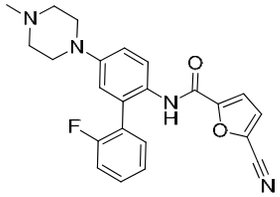

Moecule-18
IC_{50} = 890 nM

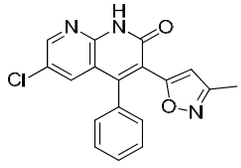

Moecule-19
IC_{50} = 1000 nM

Dataset Preparation

A set of 118 CSF1R inhibitors with an activity range (IC_{50} 0.4-2100 ηM) were collected from references[7-10]. The 3D structures of all molecules were built using Discovery Studio 3.0 (DS 3.0) (Accelrys Inc., San Diego, USA)[11]. The 3D structures of molecules were subjected to energy minimization using the Smart minimizer algorithm with a convergence gradient value of 0.001 kcal/mol. The lowest energy conformation of each molecule was further subjected conformational search using Monte Carlo like algorithm together with poling[12-14] to generate a maximum of 250 conformers. Our models emphasized a conformational diversity within the constraint of a 20 kcal/mol energy threshold above the estimated global minimum based on use of the CHARMM force field[15]. The molecules associated with their conformations were used in the pharmacophore model generation and validation.

Generation of Analogue-Based Pharmacophore Model

Quantitative pharmacophore model

The dataset of 118 CSF1R inhibitors were divided into training set (1-19, scheme-1) and test set (20-118, scheme-2 supporting information), by considering both structural diversity and wide coverage of the activity range. Training set was used for pharmacophore model generation and test set was used for validation of the pharmacophore model. The pharmacophore model was generated using '3D QSAR pharmacophore generation' module implemented in Discovery Studio 3.0.

The correct choice of the compounds in the training set is a very important in pharmacophore generation process. Because during pharmacophore generation, it enumerates all possible pharmacophore configurations using all combinations of pharmacophore features for each of the conformations of the two most active compounds.

An initial analysis revealed that chemical features such as H bond acceptor (A), H bond donor (D) and Hydrophobic aliphatic (HYali), Hydrophobic aromatic (HY aromatic) , Hydrophobic could effectively map all critical features of all molecules in training set. These features were selected to build a series of hypotheses using default uncertainty value 3. These compounds are determined by performing a simple calculation based on the activity and uncertainty.

During the 3D QSAR pharmacophore generation, it identifies features that are common to the active compounds but excludes common features for the inactive compounds within conformation tolerable regions of space. Ten hypotheses were generated for each 3D QSAR pharmacophore generation run from which the one with the highest correlation values were considered. The selected pharmacophore model was validated using cost analysis and test set activity prediction. The best pharmacophore (Hypo 1) having highest correlation coefficient (r^2), lowest total cost, and lower RMSD value was chosen to estimate the activity of test set.

Pharmacophore validation

The pharmacophore model obtained from the training set should be statistically considerable, and it should calculate the activity of the molecules exactly and be supposed to identify active compound from a given database. Therefore, the resultant pharmacophore model was validated using (i) cost analysis and (ii) test set prediction.

(i) ***Cost analysis:*** 3D QSAR pharmacophore generation identifies the best hypotheses from the many possibilities by applying cost analysis. During the model generation, it considers and rejects thousands of pharmacophore models. The overall cost of each hypothesis is calculated by summing three cost factors (i) weight cost, (ii) error cost, and (iii) configuration cost.

The weight cost is a value that increases in a Gaussian form as the feature weight in a model deviates from an idealized value of 2.0. Fixed cost (ideal cost), which represents the simplest model that fits all data absolutely. Null cost (no correlation cost), which represents the highest cost of a pharmacophore with no features and estimates activity to be the average of the activity data of the training set molecules. A meaningful pharmacophore hypothesis may result when the difference between null and fixed cost value is large; a value of 40-60 bits for a pharmacophore hypothesis may indicate that it has 75-90% probability of correlating the data. Configuration cost or entropy cost, which depends on the complexity of the pharmacophore hypothesis space and should have a value < 17. The root mean square differences (RMSD) represents the correlation between the estimated and the actual activity of the compounds.The best pharmacophore model has highest cost difference, lowest RMSD, and best correlation coefficient.

(ii) ***Test set activity prediction:*** The pharmacophore model obtained from training set is validated by predicting the activity of test set compounds. Test set is generated by 99 compounds. The best pharmacophore model having correlation coefficient (r^2), lowest total cost, and lower RMSD value was chosen to predict the activity of test set.

(iii) ***Database generation and screening:*** Database screening or virtual screening is an important computational technology, which is widely engaged

in drug discovery and development processes[16]. Virtual screening (VS) is an increasingly used method to guide the identification of novel hits from large chemical libraries. VS can be divided into two broad categories, namely ligand-based and structure-based[17]. Ligand-based approaches utilize structure activity data from a set of known actives in order to identify candidate compounds for experimental evaluation. Structure-based VS, on the other hand, utilizes the three-dimensional (3D) structure of the biological target. Here in this study we employed ligand-based approaches followed by glide docking to identify potent compounds against CSF1R. In this approach we screened Asinex database using screen 3D database protocol in DS 3.0.

In this study, we have employed ligand-based virtual screening to discover novel CSF1R drug-like molecules. Ligand-based pharmacophore model was used as 3D-search query to retrieve novel compounds from the Asinex database. For this, the best/flexible search method of Discovery Studio 3.0 was applied to retrieve compounds from the databases. A molecule must fit all the features of a pharmacophore query to be retrieved as a hit. The hit compounds can be ranked according to the fit value or estimated activity. Finally, the compounds with good fit value are then docked with crystal structure of CSF1R to further filter potential hits.

Molecular Docking

The docking studies were performed using Glide (Grid-based Ligand Docking with Energetics) 5.7 program in Schrodinger Software Suite, 2011 (Schrodinger, Portland, USA)[18]. In Glide, the initial filters test the spatial fit of the ligand to the defined active site, and examine the complementarity of ligand-receptor interactions using a grid-based method patterned after the empirical ChemScore function. Poses that pass these initial screens enter the final stage of the algorithm, which involves evaluation and minimization of a grid approximation to the OPLS-AA non-bonded ligand-receptor interaction energy. Final scoring was then carried out on the energy-minimized poses. By default, Schrodinger's proprietary Glide Score multi-ligand scoring function is used to score the poses. Emodel which is used to rank the poses, combines Glide Score, the non-bonded interaction energy, and, for rigid docking, the excess internal energy of the generated ligand conformation[19-21].

(i) ***Protein preparation:*** X-ray crystal structure of CSF1R (PDB ID: 3DPK with a resolution of 1.95 Å) was used in the docking studies. Protein preparation and minimization of hydrogen's was performed using Protein preparation wizard workflow present in Schrödinger. The protein active site analyzed carefully and tautomeric states of histidine residues, orientations of hydroxyl groups and protonation states of basic and acidic residues were done manually. Hydrogen atoms were added to the protein, and the hydrogen atoms were optimized and minimized to RMSD of 0.3 Å. The protein obtained from the Protein preparation wizard workflow used for docking.

(ii) ***Receptor grid generation*****:** Docking simulations were performed using Glide program with OPLS-AA force field. The binding region was defined using a grid of 14 Å X 14 Å X 14 Å box centered on the centroid of the overlaid crystal ligand onto the modeled 3D structure of protein, in order to confine the centroid of the docked inhibitor. Default settings were used for all the remaining parameters.

(iii) ***Ligand docking*****:** Ligand docking is done taking the prepared protein and ligands as inputs. Standard-precision (SP) docking is performed in this study. Conjugate gradient method (100 steps) was used for energy minimization of poses which had passed through the selection of initial poses scoring phase. Top 20 poses were generated per each input ligand.

Table 1 Experimental activities and pharmacophore predicted activities of training set molecules

Comp.	Exp. Activity (ηM)	Predicted Activity (ηM)	Fit value
1	0.3	3.7	6.5
2	0.4	0.14	7.92
3	0.9	4	6.47
4	2	2.7	6.63
5	3	14	5.92
6	6	13	5.97
7	7	22	5.74
8	11	2.9	6.61
9	21	25	5.67
10	38	9.9	6.07
11	52	26	5.66
12	80	19	5.79
13	90	65	5.26
14	100	55	5.33
15	140	880	4.13
16	470	170	4.84
17	630	280	4.62
18	890	310	4.58
19	1000	880	4.12

Table 2 Results of pharmacophore hypothesis generated using training set against CSF-1R inhibitors

Hypo no.	Total cost	Cost -difference	Error cost	RMSD	Correlation	Features
1	86.83	52.52	75.01	1.08	0.878	A,A,Z,Y
2	87.52	51.83	75.69	1.11	0.87	A,A,Z,Y
3	89.68	49.67	77.19	1.18	0.854	A,A,Z,Y
4	90.61	48.74	78.7	1.24	0.833	A,A,Z
5	90.81	48.54	79.01	1.26	0.829	A,A,Z,Y
6	91.09	48.26	79.2	1.26	0.827	A,A,Y
7	91.49	47.86	79.59	1.28	0.822	A,A,A,Y
8	91.51	47.84	79.72	1.29	0.82	A,A,A,Z
9	91.78	47.57	79.81	1.29	0.82	A,Z,Y
10	92.15	47.2	80.31	1.31	0.813	A,Z,Y

Results and Discussion

Quantitative pharmacophore model genration and validation

The top 10 pharmacophore models was generated using 19 CSF1R inhibitors of training set compounds by 3D QSAR pharmacophore generation module, Discovery Studio 3.0. The experimental and predicted CSF1R inhibitory activities of the 19 compounds are listed in Table 1. Cost of the null hypothesis for all 10 hypotheses is 139.35, and the fixed cost is 75.69 and the configuration cost is 10.66. A difference of 63.66 bits obtained between fixed and null costs is a sign of highly predictive nature of hypotheses. All 10 hypotheses generated showed high correlation coefficient between experimental and predicted IC_{50} values, in the range of 0.87 to 0.81 and moreover, these are having cost difference greater than 45 bits between the cost of each hypothesis and the null cost. It indicates that all the hypotheses are having true correlation between 75-90% . The cost values, RMSD and pharmacophore features are listed in Table 2.

Pharmacophore model consists of spatial arrangement of four chemical features, two hydrogen-bond acceptors (HBA), one hydrophobic aliphatic (HYali) feature, and one hydrophobic aromatic (HYaromatic) feature (Figure 1). the top active compound (1) of the training set mapped all the features are perfectly on to the features of Hypo 1 and had a fit score of 6.5, shown in (Figure 2a) whereas, for the least active compound (19) only two features of Hypo 1 were mapped properly and had fit value of 4.12, shown in (Figure 2b). These results conclude that Hypo 1 is the best ranking pharmacophore among the 10 hypotheses obtained. The mapping of pharmacophore with high active copound as depicted from the Figure (1), the one hydrogen bond acceptor (A) feature mapped with oxygen of the oxygen in furan ring, second hydrogen bond acceptor (A) mapped with Cyno group of the compound and Hydrophibic aliphatic feature with methyl group and hydrophobic aromatic group is mapped with phenyl ring.

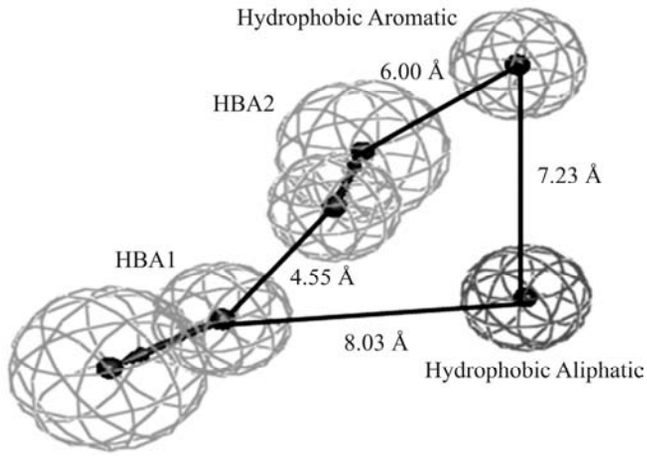

Fig. 1 Three-dimensional arrangement of pharmacophoric features in the quantitative pharmacophore model. Pharmacophore features are color-coded with green, light cyan dark cyan contours representing the hydrogen bond acceptor feature(A), hydrophobic-feature (Z) respectively. The distances between the features is in Å.

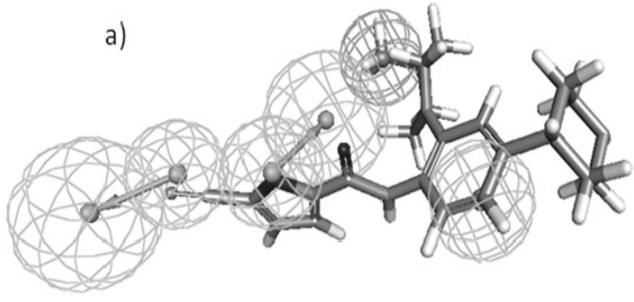

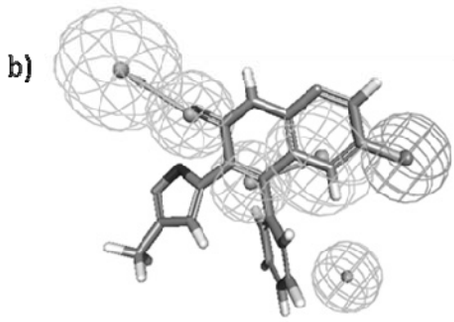

Fig. 2 Pharmacophore mapping of the most active and least compounds from the training set on the best hypothesis model Hypo 1 (a) Mapping of pharmacophore onto highly active compound-1 in training set (b) Mapping of pharmacophore onto least active compound-19 in training set.

The predictability of Hypo 1 was evaluated using a diverse test set compounds. The Hypo 1 model was predicted the activity of the 99 test set compounds and got a correlation coefficient of 0.75. Pharmacophore mapping of the highest active compound in the testset is shown in Figure 3(a) and mapping of the least active compound of the test set is shown in Figure. 3(b). The predicted activities of the compounds of the testset along with the scale were listed in the Table 3 (Supporting Information). Correlation graph between experimental and Hypo 1-estimated activities of training and test set given in Figure 4.

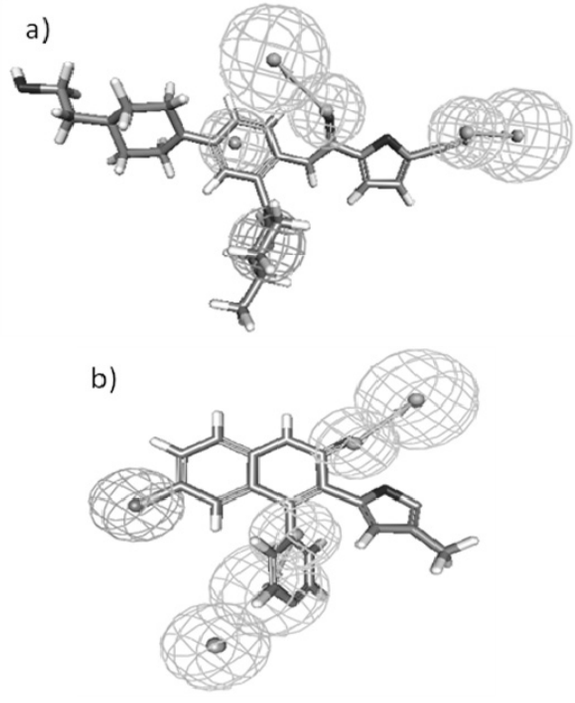

Fig. 3 Pharmacophore mapping of the most active and least compounds from the test set on the best hypothesis model Hypo 1 (a) Mapping of pharmacophore onto highly active compound-20 in test set (b) Mapping of pharmacophore onto least active compound-118 in test set.

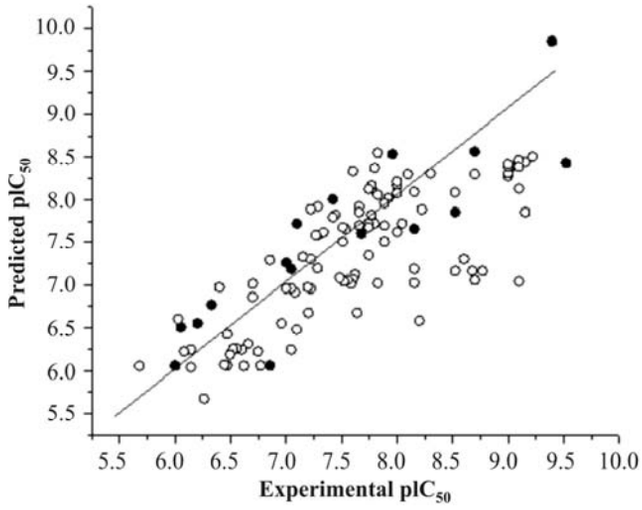

Fig. 4 Correlation graph between experimental and Hypo 1-estimated activities of training and test set.

Docking Studies

Docking studies were performed for 118 small molecule CSF1R inhibitors with the solved 3D-structure of CSF1R (PDB entry code 3DPK, 1.95 Å), using Glide module in Schrodinger. The reliability of this docking method to predict the bioactive conformation was validated using the X-ray structure of CSF1R in complex with a co-crystal molecule 8-cyclohexyl-N-methoxy-5-oxo-2-{[4-(2-pyrrolidin-1-ylethyl)phenyl]amino}-5,8-dihydropyrido[2,3-d] pyrimidine-6-carboxamide (8C5). Co-crystal 8C5 was re-docked into the active site of CSF1R and the best predicted bound conformation having lowest docking energy was selected. The superimposition of the Glide docked pose of 8C5 with the co-crystal of 3DPK is shown in Figure 5. The root mean-square deviation (RMSD) between these two poses is 0.716 Å, indicating a high docking reliability of glide in terms of reproducing the experimentally observed binding mode for CSF1R inhibitors.

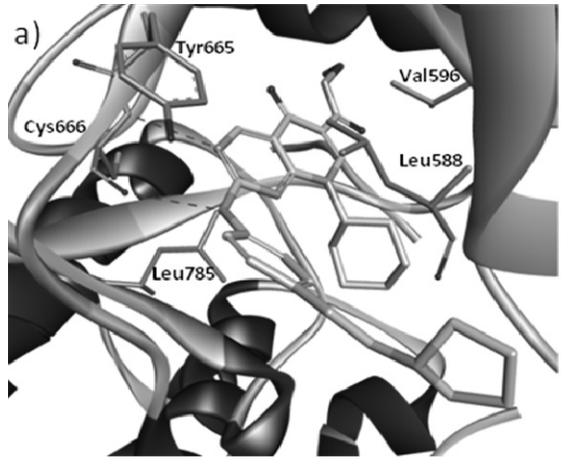

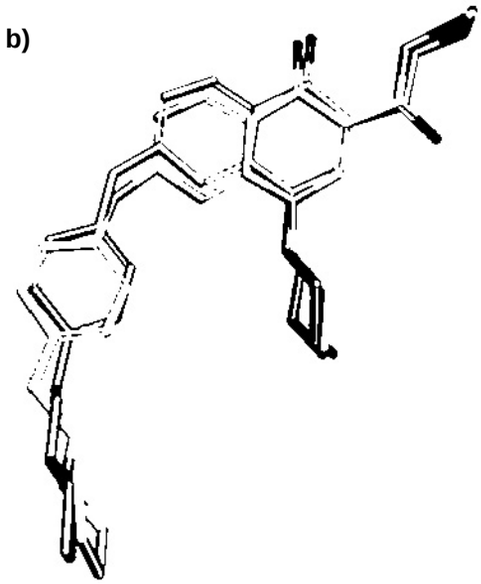

Fig. 5 (a) Predicted bound conformation of 8C5 in the active site of CSF1R (b) Superimposition of crystal ligand of 3DPK and predicted bound pose of crystal ligand generated using Glide. Crystal conformation has shown in green color and predicted bound conformation in pink colour.

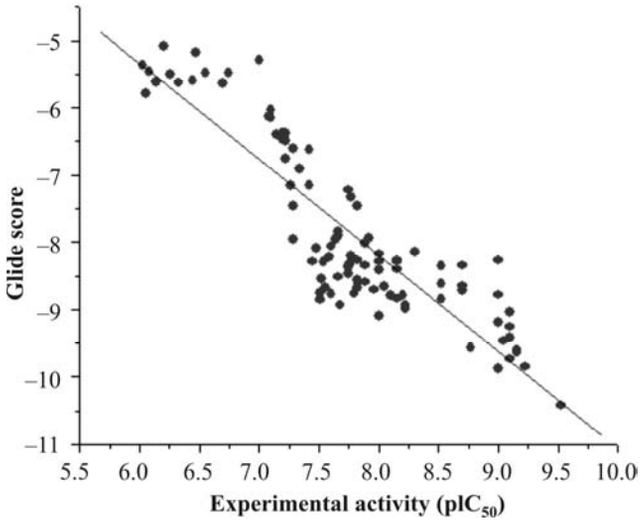

Fig. 6 Graphical representation of correlation between Glide score and experimental activity of CSF1R inhibitors.

A total set of 118 CSF1R inhibitors were docked into the active site of CSF1R and the correlation was calculated between glide sore and the IC 50 by linear regression analysis method. An acceptable correlation coefficient of ~ 0.78 was obtained between experimental IC50 and glide score (Figure 6). This correlation clearly specifies that the binding conformations of the CSF1R inhibitors in the CSF1R active site are reliable.

As shown in the Fig. 7 (a and b), the best-docked conformation of the most active compound (1) forms important hydrogen bond interactions with CSF1R active site. The first hydrogen bond is formed between the carbonyl oxygen of the core and with the main chain NH group of Cys666 (O–HN, 2.32 Å). The second hydrogen bond interaction is observed between the NH of Piperidine group of the compound with the side chain hydroxyl group of Tyr665 (NH–O, 2.65 Å). The 4-methylpiperidine group fits well in the hydrophobic pocket fromed by the Leu588, Val596, Leu795, Phe797.

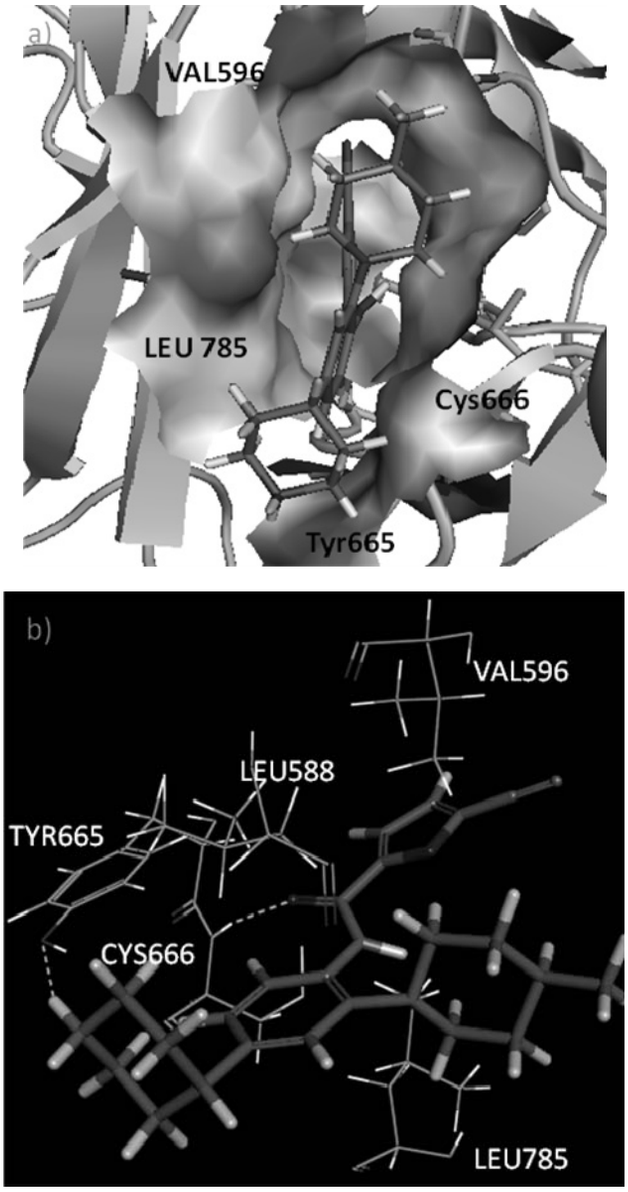

Fig. 7 (a) Binding mode of high active compound in the protein active site (b) Interaction of binding conformation in the active site.

***Virtual screening and hit selection*:** In this study we implemented pharmacophore-based virtual screening. The hits obtained from virtual screening were collected for further analysis using Glide docking to identify potent small molecules against CSF1R. The sequential workflow performed in this study is schematically represented in a flowchart in Figure 8.

The best pharmacophore model (Hypo 1) was used as a virtual screening query, to identify novel and potent compounds. Virtual screening was performed against inhouse 3D database of 20,000 compounds. A set of 5022 compounds were obtained from pharmacophore screening, a subset of these structures was created by removing all the molecules that did not satisfy the Lipinski rules, describing properties of drug-like compounds. To further amplify the possibility, only molecules that have a fit score between 7.5 and 5 were considered. These sets of 1521 molecules were docked on to the CSF1R active site using Glide SP mode. Docking was performed in order to study the binding orientation and determine productive interactions within the active site. From the docking studies. 12 hits showed high complementarity with the active site of CSF1R and this hits were selected for pharmacological screening against CSF1R. The docking interactions and pharmacophore mapping of one of the best hit BAS12532928 are shown in Figure 9 (a & b).

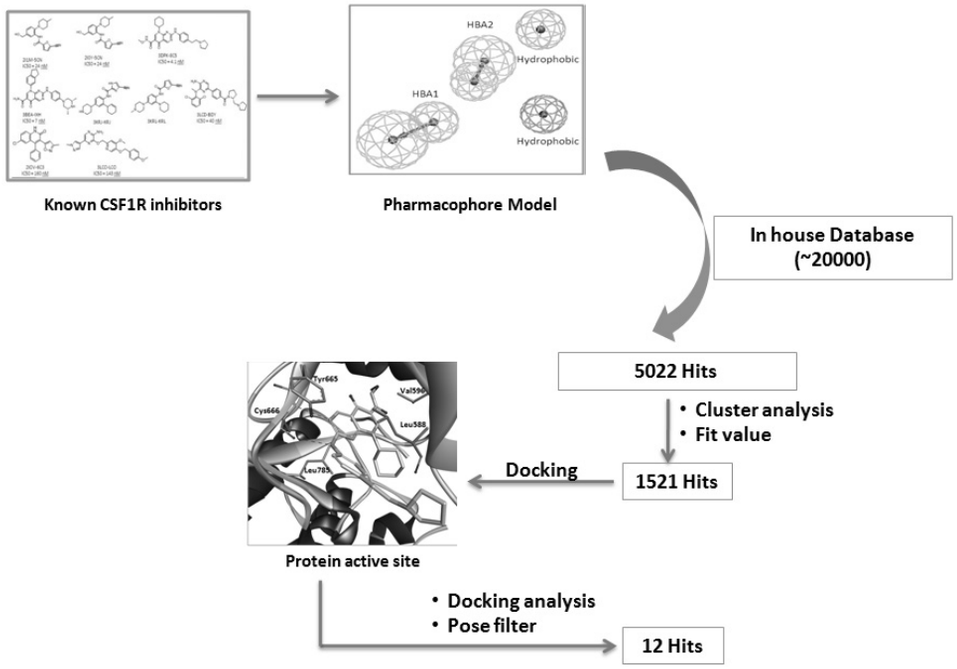

Fig. 8 Virtual Screening criteria for Identification CSF1R Inhibitors.

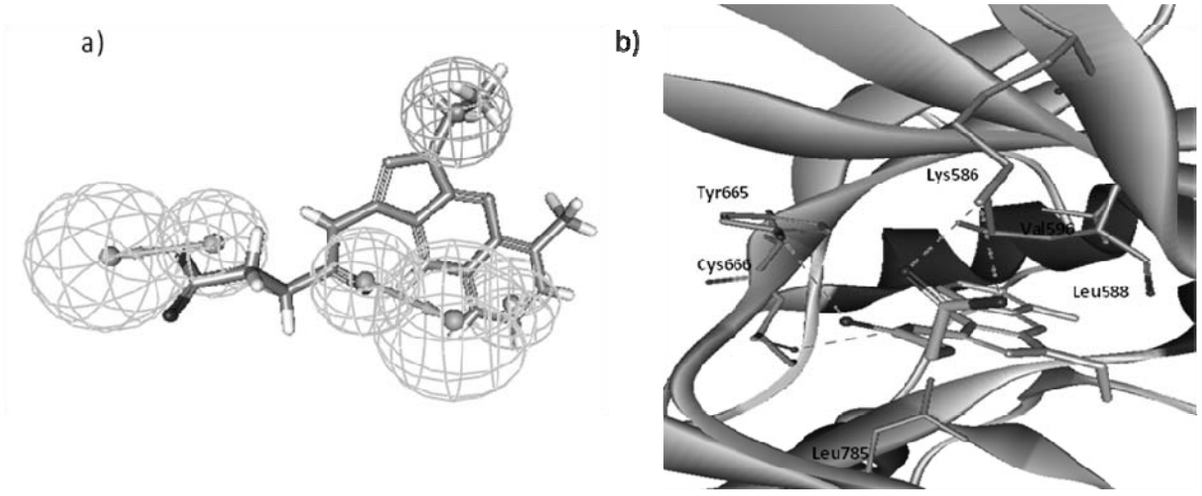

Fig. 9 (a) Pharmacophore mapping of the virtual screening hit (BAS 12532928) on the best hypothesis model Hypo 1. (b) Docked conformation of the best virtual screening hit (BAS 12532928) in the active site of CSF1R. Dashed lines represent hydrogen bonds.

Conclusion

In this study, we have discussed the identification of and potential hits against CSF1R using pharmacophore modeling. The generated model contains four features: two hydrophobic groups and two hydrogen bond acceptors. The resulting pharmacophore model was used as a 3D-search query with inhouse 3D database. The hit compounds were further prioritized using fit value and docking studies. The docking studies revealed that amino acid Cys666 and hydrophobic region are important for ligand binding. Finally, a total of 12 hits were suggested based on binding mode and the best fit value. It could be expected that the hits from this study may be potential leads for CSF1R inhibition.

References

[1] Sherr CJ, Rettenmier CW, Sacca R, Roussel MF, Look AT, Stanley ER (1985). Cell. **41:** 665-676.

[2] Stanley ER, Guilbert LJ, Tushinski RJ, Bartelmez SH (1983). *J Cell Biochem.* **21:** 151-159.

[3] Hamilton JA (2008). *Nat Rev Immunol.* **8:** 533-44.

[4] Chitu V, Stanley ER (2006). *Curr Opin Immunol.* **18:** 39-48.

[5] Pixley FJ, Stanley ER (2004). *Trends Cell Biol.* **14:** 628-38.

[6] Bourette RP, Rohrschneider LR (2000). *Growth Factors.* **17:** 155-66.

[7] Meegalla SK, Wall MJ, Chen J, Wilson KJ, Ballentine SK, Desjarlais RL, Schubert C, Crysler CS, Chen Y, Molloy CJ, Chaikin MA, Manthey CL, Player MR, Tomczuk BE, Illig CR (2008). *Bioorg Med Chem Lett.* **18:** 3632-3637.

[8] Illig CR, Chen J, Wall MJ, Wilson KJ, Ballentine SK, Rudolph MJ, DesJarlais RL, Chen Y, Schubert C, Petrounia I, Crysler CS, Molloy CJ, Chaikin MA, Manthey CL, Player MR, Tomczuk BE, Meegalla SK (2008). *Bioorg Med Chem Lett.* **18:** 1642-1648.

[9] Wall MJ, Chen J, Meegalla S, Ballentine SK, Wilson KJ, DesJarlais RL, Schubert C, Chaikin MA, Crysler C, Petrounia IP, Donatelli RR, Yurkow EJ, Boczon L, Mazzulla M, Player MR, Patch RJ, Manthey CL, Molloy C, Tomczuk B, Illig CR (2008). *Bioorg Med Chem Lett.* **18:** 2097-2102.

[10] Scott DA, Balliet CL, Cook DJ, Davies AM, Gero TW, Omer CA, Poondru S, Theoclitou ME, Tyurin B, Zinda MJ (2009). *Bioorg Med Chem Lett.* **19:** 697-700.

[11] Discovery Studio, Accelrys package, version 3.0, Available from: www. accelrys.com.

[12] Andrew Smellie, Steven L. Teig, Peter Towbin (1995). *J. Comput. Chem.* **16:** 171-187

[13] Andrew Smellie, Scott D. Kahn, Steven L. Teig (1995). *J. Chem. Inf. Comput. Sci.* **35:** 285-294.

[14] Andrew Smellie, Scott D. Kahn, Steven L. Teig (1995). *J. Chem. Inf. Comput. Sci.* **35:** 295-304.

[15] Brooks B.R, Bruccoleri R.E, Olafson B.D, States D. J, Swaminathan S, Karplus M (1983). *J. Comput. Chem.* **4:** 187-217.

[16] Walters W.P, Stahl M.T, Murcko M.A (1998). Virtual Screening-An Overview. *Drug Discov. Today* **3:** 160-178.

[17] Mestres J, Knegtel R.M.A (2000). *Perspect. Drug Des. Discovery* **20:** 191-207.

[18] Suite 2011: Glide, version 5.7, Schrödinger, LLC, New York, NY, 2011.

[19] Eldridge M. D, Murray C. W, Auton T. R, Paolini G. V, Mee R. P (1997). *J. Comput.-Aided Mol. Des.* **11:** 425-445.

[20] Friesner R. A, Banks J. L, Murphy R. B, Halgren T. A, Klicic J. J, Mainz D. T, Repasky M. P, Knoll E. H, Shaw D. E, Shelley M, Perry J. K, Francis P, Shenkin P. S (2004). *J. Med. Chem.* **47:** 1739-1749.

[21] Friesner R. A, Murphy R. B, Repasky M. P, Frye L. L, Greenwood J. R, Halgren T. A, Sanschagrin P. C, Mainz D. T (2006). *J. Med. Chem.* **49:** 6177-6196.